nature neuroscience

A representation of the hazard rate of elapsed time in macaque area LIP

Peter Janssen[1,2] & Michael N Shadlen[1]

The capacity to anticipate the timing of environmental cues allows us to allocate sensory resources at the right time and prepare actions. Such anticipation requires knowledge of elapsed time and of the probability that an event will occur. Here we show that neurons in the parietal cortex represent the probability, as a function of time, that a salient event is likely to occur. Rhesus monkeys were trained to make eye movements to peripheral targets after a light dimmed. Within a block of trials, the 'go' times were drawn from either a bimodal or unimodal distribution of random numbers. Neurons in the lateral intraparietal area showed anticipatory activity that revealed an internal representation of both elapsed time and the probability that the 'go' signal was about to occur (termed the hazard rate). The results indicate that the parietal cortex contains circuitry for representing the time structure of environmental cues over a range of seconds.

Humans and animals rely on a sense of elapsed time to plan actions, anticipate salient events, infer causal regularities and learn associations[1]. Yet little is known about the neural mechanisms that underlie the encoding and use of elapsed time[2,3]. Traditionally, the focus has been on the cerebellum and basal ganglia, but several recent studies suggest that the association areas of the neocortex may play an important role[4–6]. Neurons in association areas perform computations that span gaps in time between sensation and action in order to mediate working memory[7], motor planning[8,9] and decision making[10–12]. These processes depend on a representation of time to infer temporal order, plan sequences of actions and control the tradeoff between speed and accuracy. In general, processes not controlled by immediate external events may still need to know when information is useful.

Behavioral performance is enhanced if subjects can anticipate the point in time that a stimulus is likely to appear or an instruction is likely to occur[4,13–15]. To anticipate the timing of behaviorally relevant events, the brain must represent the passage of time and use this representation to estimate the probability that an event is likely to occur, given that it has not occurred already. This computation is termed a hazard rate[14].

Although several brain regions have been shown to encode the probability that an action will ensue[12,16,17], little is known about how such probabilities are represented by the brain when they change as a function of time. Neurons in various brain areas have occasionally shown climbing activity in the interval preceding a test stimulus or 'go' instruction, an effect that has been interpreted as a neural correlate of anticipation[18–23]. A recent study showed that neurons in the lateral intraparietal area (LIP) undergo time-dependent changes in their responses when monkeys make decisions about the duration of a time interval[5]. Because LIP neurons show sustained changes in firing rate during delayed eye movement tasks[9,24–26], we hypothesized that this persistent activity might encode the hazard rate used to anticipate the time of a pending 'go' signal.

RESULTS

Two rhesus monkeys were trained to make eye movements to a peripheral target (**Fig. 1a**). The monkeys were required to hold steady fixation until the fixation spot had dimmed and were then rewarded for initiating an accurate eye movement as soon as possible (see Methods). The waiting time between target onset and the 'go' signal (that is, the 'go' time) was a random variable whose probability distribution was fixed throughout a block of trials. We used two time schedules in alternating blocks of trials. In the bimodal time schedule (**Fig. 1b**, top row left), the 'go' signal could come either early or late, but not in the interval between 0.75 and 1.75 s, whereas in the unimodal time schedule (**Fig 1b**, top row right), the 'go' times were distributed between 0.5 and 2 s.

We reasoned that exposure to these schedules might allow the monkeys to anticipate the arrival of the 'go' signal. The time course of such anticipation is formalized by the hazard rate. Because the brain cannot estimate elapsed time precisely[1], the mathematical functions are replaced by blurred versions, which we term subjective hazard rates or anticipation functions (see Methods). There are clear differences between the anticipation functions associated with the unimodal and bimodal schedules (**Fig. 1b**, bottom). When 'go' times are drawn from the unimodal distribution, the anticipation function mainly increases with waiting time. In contrast, when 'go' times are drawn from the bimodal distribution, the anticipation is triphasic: it rises, falls and

[1]Howard Hughes Medical Institute, National Primate Research Center and Department of Physiology and Biophysics, University of Washington, Box 357290, Seattle, Washington 98195. [2]Present address: Laboratorium voor Neuro-en Psychofysiologie, KU Leuven Medical School, Herestraat 49, B-3000 Leuven, Belgium. Correspondence should be addressed to M.N.S. (shadlen@u.washington.edu).

Published online 16 January 2005; doi:10.1038/nn1386

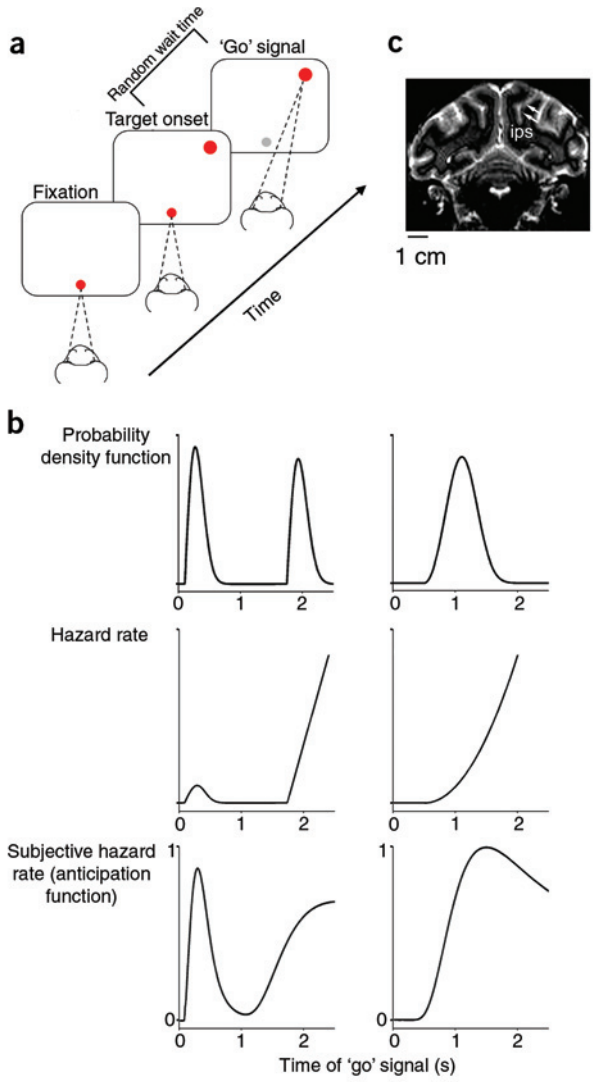

Figure 1 Methods. (**a**) Delayed eye movement task. The monkey made eye movements to the red target as soon as the fixation point dimmed. The target appeared in different locations on each trial. Here we report trials in which the target appeared in the response field of the LIP neuron we recorded. A bracket demarcates the random waiting time between target onset and 'go' signal. (**b**) Probability distributions, hazard rates and subjective hazard rates. The top row illustrates the probability distributions for drawing 'go' times under the two schedules used in the experiments: bimodal (left) and unimodal (right). The middle row shows the hazard rates for each of these time schedules (equation (3)). The bottom row shows the subjective hazard rates or anticipation functions for each of these time schedules ($A_b(t)$ and $A_u(t)$, $\phi = 0.26$, equation (4)). The functions employ a common scale, which is normalized to the peak of the $A_u(t)$. (**c**) Representative magnetic resonance image from monkey J. Neurons in both monkeys were recorded from the posterior portion of LIPv[27], outlined by the arrows; ips, intraparietal sulcus.

rises again. The scale of these anticipation functions was set from 0 to 1 to facilitate interpretation of the behavioral and physiological data, as described below.

Anticipation of the 'go' cue affects saccade reaction time

Both monkeys learned to anticipate the time of the 'go' signal, as evidenced by their reaction times. **Figure 2** shows running means of reaction times measured under the unimodal (purple) and bimodal (red) schedules. Each point shows the mean of 51 observations. In both types of blocks, reaction time showed a clear dependency on the amount of time that elapsed before the 'go' signal. In 'unimodal schedule' blocks, reaction time decreased with longer waiting times (regression analysis, $P < 0.001$). In 'bimodal schedule' blocks, reaction time decreased and rose again for 'go' times that happened to be drawn from the first mode and was fastest for 'go' times that were drawn from the second mode. This triphasic pattern was more striking for monkey J (**Fig. 2a**), but it was evident in both monkeys, as shown below. The reaction times from both monkeys clearly decreased between the early and later modes (for monkey J, mean reaction time was 268 ± 1.2 and 237 ± 0.8 ms in epochs within ±350 ms of the first and second modes, respectively; for monkey H, the corresponding means were 295 ± 0.7 and 259 ± 1).

The monkeys' reaction times were inversely related to the anticipation functions associated with the schedules of random 'go' times. For either schedule, the data were well fit by a weighted sum of the two anticipation functions delayed by 56 ms (Methods, equation (5)). These fits furnish estimates of the number of milliseconds that reaction time is reduced per unit change in anticipation (**Table 1**). Under the bimodal schedule, the fit to the data from monkey J (**Fig. 2a**) is dominated by the bimodal anticipation function, whereas under the unimodal schedule, the fit is dominated by the unimodal anticipation function (**Table 1**). For monkey H, the unimodal anticipation function explains most of the decline in reaction time under both schedules. Nevertheless, the bimodal anticipation function has a significant role under the bimodal schedule of 'go' times ($P < 0.02$); (**Table 1**).

The influence of the bimodal anticipation function can be understood more directly by examining the partial correlation between the reaction times from individual trials and the anticipation function appropriate for the schedule. Because both anticipation functions can affect the pattern of reaction times under either schedule, we performed a partial (conditional) correlation to factor out the influence of the potentially confounding anticipation function. Under the bimodal schedule, the partial correlation between reaction time and the bimodal anticipation function, $r_{RT_b,A_b|A_u}$, was –0.36 for monkey J ($P < 0.001$, Fisher z). Under the unimodal schedule, there was a significant inverse correlation between reaction time and the unimodal anticipation function ($r_{RT_u,A_u|A_b} = -0.24$; $P < 0.001$). A similar inverse correlation was present

Table 1 Weighting coefficients for the unimodal and bimodal anticipation functions fit to reaction time data in **Figure 2**, using equation (5)

	Weights of anticipation functions fit to reaction times (ms change in reaction time per unit anticipation)					
	Monkey J			Monkey H		
Distribution of 'go' times	w_u	w_b	R^2	w_u	w_b	R^2
Bimodal schedule	–42.2 ± 1.4	–69.8 ± 4.2	0.96 (0.29)	–40.0 ± 2.0	–9.7 ± 3.9	0.95 (0.39)
Unimodal schedule	–17.9 ± 2.2	–9.7 ± 6.9*	0.77 (0.06)	–32.9 ± 2.6	–22.1 ± 9.1	0.91 (0.11)

The coefficients multiply the anticipation functions, $A_u(t)$ and $A_b(t)$. One unit of anticipation is the range of $A_u(t)$ shown in **Figure 1**. Both anticipation functions affected reaction time inversely under both schedules ($P < 0.02$, except for asterisk). R^2 describes the fraction of the running mean variance explained by the fit; parenthetical values describe the fraction of variance for individual trials.

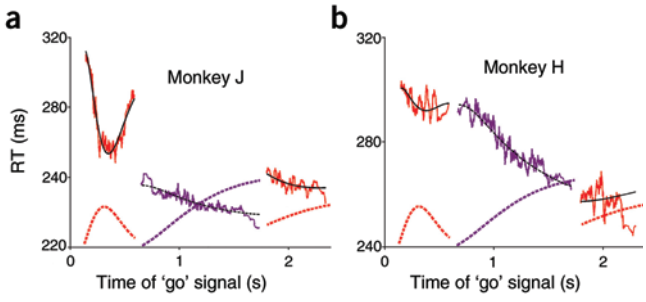

Figure 2 Reaction time (RT) is modulated by anticipation of the 'go' cue. Eye movement RTs are plotted as a function of the waiting time between target onset and the 'go' signal (the 'go' time), during the bimodal (red) and the unimodal (purple) time schedules. Points represent running means of RT from 51 consecutive 'go' times. Black curves are fits to the data using a weighted sum of the anticipation functions (equation (5); weights are in **Table 1**). The dashed red curve is the bimodal anticipation function sampled at the 'go' times that occur under the bimodal schedule. The dashed purple curve shows the unimodal anticipation function sampled at the 'go' times under the unimodal schedule. Note that RTs are only measured when there is a finite probability that a 'go' cue could occur. (**a**) Data from monkey J ($n = 2{,}322$ unimodal trials and $n = 1{,}876$ bimodal trials). (**b**) Data from monkey H ($n = 1{,}480$ unimodal trials and $n = 1{,}456$ bimodal trials).

in monkey H ($r_{RT_b,A_b|A_u} = -0.09$; $r_{RT_u,A_u|A_b} = -0.32$; $P < 0.001$ for both values). These behavioral observations imply that the brain is capable of representing both the passage of time and the time-dependent probability that the 'go' signal is about to occur.

Anticipation of the 'go' cue affects LIP neural activity

We recorded 70 LIP neurons, screening them using an eye movement task in which monkeys made saccadic eye movements to the remembered location of a briefly flashed target. We studied only those neurons that showed strong, spatially selective activity during the memory period between the flashed eye movement target and the 'go' instruction (see Methods). These neurons were commonly encountered in the ventral portion of LIP[27] (**Fig. 1c**). We then tested these neurons using the delayed saccadic eye movement task with a bimodal or unimodal distribution of random 'go' times. In half the trials, the saccade target was in the response field of the LIP neuron, giving rise to a persistent elevation in the neural activity. Our focus is on the modulation of this persistent activity while the monkey awaited the 'go' instruction.

Many neurons in area LIP altered their firing rates as a function of time, in accordance with the changing anticipation of the 'go' signal. **Figure 3a** shows responses of a representative neuron recorded in blocks of trials using either the bimodal or the unimodal schedule of 'go' times. Each curve represents averaged spike rates measured during

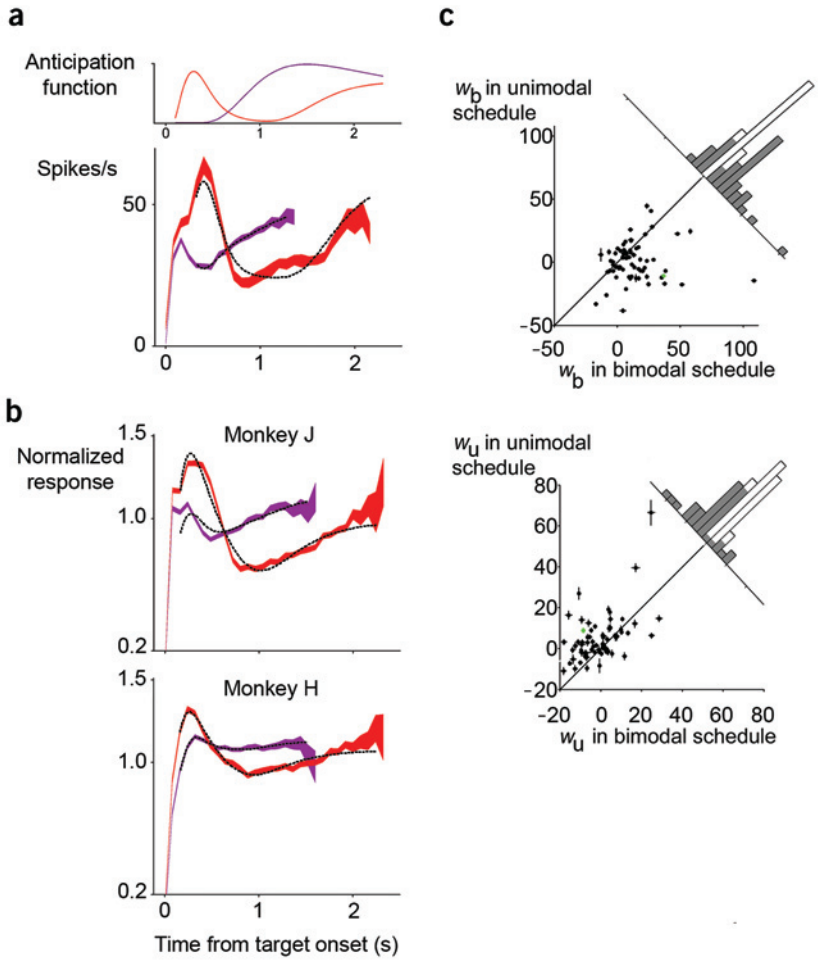

Figure 3 LIP responses represent anticipation as a function of time. (**a**) Single-neuron example. Top: anticipation functions for the unimodal (purple) and the bimodal (red) time schedule. Bottom: average neural activity recorded during waiting period for the 'go' signal under the bimodal (red) and the unimodal (purple) time schedule. Shading, s.e.m.; black curves, fits to equation (5). (**b**) Population responses from blocks using bimodally and unimodally distributed 'go' times. Averaged normalized responses (± s.e.m.) plotted as a function of waiting time for monkey J ($n = 39$) and monkey H ($n = 31$). Spike rates from each neuron were normalized to the mean activity 320–1,360 ms after target onset using all trials in both schedules. Black curves, fits to equation (5); red, bimodal schedule; purple, unimodal schedule. (**c**) Effect of schedule on the temporal pattern of the response from single neurons. Average response from a block using either bimodal or unimodal schedule of 'go' times was described as a weighted sum of anticipation functions, $A_u(t)$ and $A_b(t)$. Upper scatter plot compares amount of response modulation attributed to $A_b(t)$ in unimodal and bimodal testing blocks. The bimodal anticipation function explained more of the response modulation during the block of trials using bimodally distributed 'go' times (mean w_b was +14.1 and +0.8 during the bimodal and unimodal schedules, respectively). Differences are summarized by the frequency histogram. Lower scatter plot compares amount of response modulation attributed to $A_u(t)$ in unimodal and bimodal testing blocks. The unimodal anticipation function explained more of the response modulation during the block of trials using unimodally distributed 'go' times (mean w_u was +4.8 and –1.1 during unimodal and bimodal schedules, respectively). Differences are summarized by the frequency histogram. Error bars, s.d. of parameter estimates. Shaded histograms indicate significant cases, $P <$ 0.01. Green symbols indicate example neuron in **a**.

Table 2 Weighting coefficients for the unimodal and bimodal anticipation functions fit to response averages in **Figure 3b**, using equation (5)

	Weights of anticipation functions fit to LIP response (Percentage change in firing rate per unit anticipation)			
	Monkey J		Monkey H	
Distribution of 'go' times	w_u	w_b	w_u	w_b
Bimodal schedule	–19 ± 1	+51.4 ± 1.9	–7.1 ± 1.8	+39 ± 2.7
Unimodal schedule	+25 ± 2	+26 ± 2.3	+11 ± 1.4	+22 ± 2.3

The coefficients multiply the anticipation functions, $A_u(t)$ and $A_b(t)$. Units for the population responses are percentage change in firing rate (relative to the average delay period activity) per unit change in the anticipation function. One unit of anticipation is the range of $A_u(t)$ shown in **Figure 1b**. Schedule affected the weights in the appropriate direction (compare weights in each column; $P < 10^{-5}$ for all comparisons).

the waiting period from the onset of the eye movement target at the cell's preferred location until the dimming of the fixation point.

When the neuron was studied in a bimodal 'go' time schedule, the firing rate showed an early peak in activity at ~0.4 s after target onset. Then, if the 'go' signal did not arrive, the activity declined by 41 spikes s^{-1} over the following 0.4 s. Then, from ~0.8 s, the response increased gradually by 24 spikes s^{-1} as the monkey awaited a 'go' signal drawn from the later mode of the bimodal distribution. When the neuron was studied with a unimodal 'go' time schedule, the early rise in activity was conspicuously absent. After the onset response, the firing rate declined by 9 spikes s^{-1} until ~0.4 s, and then increased steadily by 20 spikes s^{-1} from 0.4 to 1.4 s as the monkey waited for the 'go' signal to arrive.

The time course of activity from this neuron was strongly influenced by the monkey's knowledge of the random 'go' time schedule. Notably, the responses depicted by the purple and red curves in **Figure 3a** were recorded under identical physical conditions: while viewing the same target and fixation point and awaiting the 'go' signal. The marked difference in the time course of the neural response reflects only a difference in the monkey's state of anticipation.

The response functions in **Figure 3a** can be approximated by a weighted sum of the anticipation functions associated with the unimodal and bimodal schedules (black curves). The weights derived from these fits furnish a test of the hypothesis that the LIP response is dominated by the hazard function associated with the schedule that the monkey experienced. For the neuron in **Figure 3a**, the weights assigned to the bimodal and unimodal anticipation functions (w_b and w_u, respectively) were +36.6 ± 1.7 and –8.6 ± 1.1, respectively, during testing with the bimodal schedule. In contrast, during testing with the unimodal schedule, the fit was dominated by the unimodal anticipation function: $w_b = -10.7 \pm 1.3$, $w_u = +8.9 \pm 1.3$. The negative weights associated with the 'wrong' anticipation function suggest that LIP activity also reflects the knowledge that under each of the schedules certain 'go' times will not occur.

These weighting coefficients estimate the change in spike rate associated with the range of the anticipation functions shown in **Figure 3a** (top); they have the unit 'spikes per second per unit of anticipation', where one unit is the range of the subjective hazard associated with the unimodal distribution (see Methods). The weights and their standard errors demonstrate that the response modulations observed in either block are dominated by the appropriate bimodal or unimodal anticipation function.

Figure 3b shows the averaged responses from all 70 neurons in the two monkeys. To make these graphs, we normalized the responses from each neuron to its average firing rate during the delay period using combined data from both schedules. When the 'go' times were drawn from a bimodal distribution, the response averages showed a triphasic pattern: increasing in anticipation of 'go' times drawn from the early mode, then decreasing when 'go' signals were unlikely to occur, then increasing again in anticipation of 'go' times drawn from the later mode (**Fig. 3b**, red). When the 'go' times were drawn from the unimodal distribution, the triphasic pattern was less apparent. The responses showed a steady rise (monkey J) or remained stable (monkey H) from ~0.4 s onward.

The graphs demonstrate that anticipation-related modulation can constitute a large fraction of the delay period activity. For example, during the waiting period for bimodally distributed 'go' signals, the responses from monkey J modulated between –40% and +40% of the delay period activity (**Fig. 3b**, upper red curve). These effects were smaller in monkey H, but the effect of schedule on the responses was highly significant for both monkeys. Fits to the response averages using weighted sums of the anticipation functions (equation (5); **Fig. 3**, black curves) indicate that the schedule affected the pattern of firing in both monkeys (**Table 2**). When the schedule changed from unimodal to bimodal, the fitted response functions showed an increase in the weight of the bimodal anticipation function on the response and a decrease in the weight of the unimodal schedule ($P < 10^{-5}$ for all comparisons in both monkeys; see **Table 2**).

Individual neurons showed a variety of response patterns, but most underwent modulations similar to the response averages and example in **Figure 3a**,**b**. The spike rate functions for 68 of 70 neurons (97%) were well described by a weighted sum of the two anticipation functions ($P < 0.05$; H_0: $w_b = w_u = 0$; mean $R^2 = 0.67$; interquartile range = 0.53–0.87) delayed by 55 ms on average (τ, equation (5)). The scatter plot in the upper panel of **Figure 3c** compares the contribution of the bimodal anticipation function to each neuron's response under the two schedules. This bimodal anticipation function was weighted significantly more during the block using the bimodal schedule of 'go' times (mean difference = +12.2 ± 2.8, $P < 0.001$, paired t-test). The corresponding analysis of the unimodal anticipation functions is shown in the lower panel of **Figure 3c**. The unimodal anticipation functions tended to exert less weight overall but were stronger during blocks of trials using the unimodal schedule of 'go' times (mean difference = –5.9 ± 1.3, $P < 0.01$).

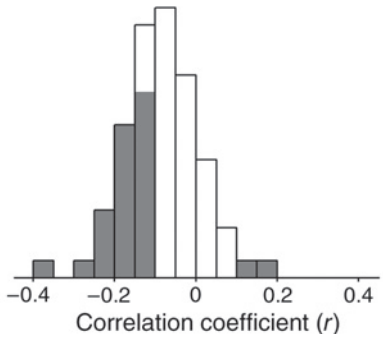

Figure 4 Neural activity is inversely related to reaction time on a trial-by-trial basis. For each trial, we compared the reaction time to the neural activity in an epoch from 150 ms before to 50 ms after the 'go' signal. We removed the potentially confounding effect of time by subtracting the mean reaction time and spike rate from each value. The correlation coefficient was obtained using these residual values. The histogram shows r-values from 70 cells (shading indicates significance; $P < 0.05$ in 28/76 neurons; Fisher z) using all trials from unimodal and bimodal schedules (results are similar using either schedule alone). The weak but significant inverse correlation indicates that variability in neural activity in LIP affects the reaction time.

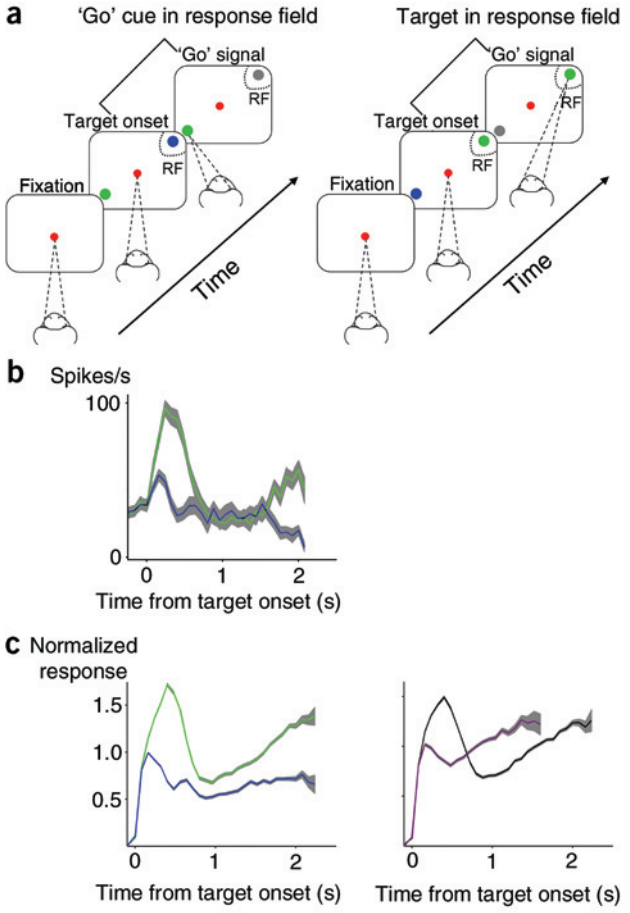

Figure 5 Time-dependent anticipatory activity is associated with motor preparation. (**a**) Variant of the delayed eye movement task. The monkey made an eye movement to the green target as soon as the blue stimulus dimmed. The monkey must attend to both targets but plan an eye movement only to the green target. Either target could appear in the neuron's response field. (**b**) Single-neuron responses. The average activity is shown for trials in which the saccade target appeared in the response field (green) and for trials in which the 'go' cue appeared in the response field (blue). (**c**) Population responses. Left, response averages from 25 neurons (monkey J) on trials in which the saccade target appeared in the response field (green) and trials in which the 'go' cue appeared in the response field (blue). Right, population responses of the same 25 neurons on trials in which both the saccade target and the 'go' signal appeared in the response field (black), along with the average activity of these 25 neurons on trials using the unimodal time schedule with the saccade target in the response field (purple).

Note that the weights for the appropriate anticipation function tended to be positive, indicating that greater anticipation leads to higher spike rates, on average, in LIP.

Together, these findings indicate that persistent activity in LIP is modulated by the passage of time. All of the neurons in our sample respond selectively to targets in their response fields. Yet, during the delay period in which the monkeys knew where but not when to make an eye movement, LIP neurons modulated their discharge by tens of spikes per second (on the order of one-third the level of sustained activity) in a pattern resembling the theoretical anticipation functions associated with the schedules of random 'go' times.

The changes in neural activity associated with the change in task timing evolved on a short time scale (on the order of minutes) and were highly flexible. For the neuron in **Figure 3a**, reliable changes in the modulation pattern emerged as early as 20 trials after the change in the time schedule. For example, w_b decreased from $+36.6 \pm 1.7$ to $+2.6 \pm 1.7$ and w_u increased from -8.6 ± 1.1 to $+22.4 \pm 2.0$ over the first 20 trials ($P < 0.001$, data not shown). Notably, this rapid change was also evident in the monkeys' behavior. As is apparent from **Figure 2a**, reaction time tended to be shorter on average under the unimodal schedule across all 'go' times. This change was apparent within 30 trials after the change from the bimodal to the unimodal time schedule in monkey J ($P < 0.01$, t-test).

To further examine this flexibility, we conducted a third block of testing in 11 neurons (monkey J) in which we reverted to the first schedule of random 'go' times used in the first block (either unimodal or bimodal). The neural activity in this third block changed again and became similar to the activity in the first block of trials. In bimodal-unimodal-bimodal sequences, w_b was +33.6, +4.2, and +18.6 spikes s^{-1} per unit anticipation, respectively. In unimodal-bimodal-unimodal sequences, w_u was +8.3, +0.1, and +6.9 spikes s^{-1} per unit anticipation, respectively.

Trial-to-trial correlation between neural activity and behavior

Does the anticipatory activity in LIP help the monkey prepare its eye movement, or are the behavioral and neural manifestations of anticipation merely coincidental? Although it is impossible to exclude the latter possibility without manipulating the discharge of the neurons we recorded, some insight can come from examining the relationship between neural activity and reaction time on single trials. We asked whether the firing rate in the epoch around the time of the 'go' signal predicted the monkey's reaction time on that trial. By subtracting the mean neural activity and mean reaction time from the data, we removed the effect of time and anticipation from both sets of measurements, leaving only the residual changes about the time-dependent means. We then calculated a correlation coefficient between these residual values for each neuron in our sample. The histogram of correlation coefficients (**Fig. 4**) shows that the majority of neurons showed a negative correlation between firing rate and reaction time on single trials (median correlation coefficient = –0.09, $P < 0.001$; for neurons with significant anticipation modulation, the median correlation coefficient was –0.10, $P < 0.001$). The size of this correlation was weak, but it is notable that the variable discharge of a single neuron on a single trial has any impact at all on the monkey's reaction time. Thus, in addition to reflecting the monkeys' state of anticipation, the time-dependent activity of LIP neurons is probably partially responsible for the behavioral manifestation of this anticipation in the saccadic eye movements.

Anticipatory activity is associated with eye movement planning

Previous studies suggest that area LIP plays a role in the allocation of spatial attention and the planning of eye movements[9,26,28]. The anticipatory activity we observed could reflect temporal variation in either of these functions. To distinguish these possibilities, we trained the monkeys on a variant of our delayed eye movement task (**Fig. 5a**). Instead of anticipating the dimming of the fixation point, the monkey was required to monitor a second peripheral target, which was distinguished by its color. The sole purpose of this second target was to provide the 'go' signal, again by dimming slightly, thereby instructing an eye movement to the other target. Thus the monkey had to attend to the 'go' cue and possibly to the saccade target, but the eye movement plan was directed only to the latter. By placing either the 'go' cue or the eye movement target in the neuron's response field, we could determine whether anticipatory activity in LIP is associated with the direction of the intended eye movement, spatial attention or both.

The neuron in **Figure 5b** showed robust anticipatory activity associated with the bimodal time schedule when the eye movement target appeared in the response field (w_b = +65.2 ± 3.6, w_u = –13.2 ± 2.2). In contrast, when the 'go' cue was in the response field, this anticipatory modulation was much weaker (**Fig. 5b**; w_b = +6.9 ± 1.8, w_u = –13.8 ± 1.0). This pattern of results was similar across the population of 25 neurons tested in this manner (**Fig. 5c**, left). The average w_b was +24.7 ± 2.5 spikes s^{-1} per unit anticipation when the target appeared in the response field compared to +5.1 ± 1.9 when the 'go' cue appeared in the response field. Although it is not apparent in the figure, the weaker representation of the bimodal anticipation function in the latter configuration was significant ($P < 0.01$, t-test). In contrast, when these neurons were tested under the unimodal schedule (target in response field), the responses did not show a positive influence of the bimodal anticipation function (**Fig. 5c**, right; mean w_b = –4.1 ± 1.2, mean w_u = +6.3 ± 0.9).

To test whether we were suppressing modulation at the attended location of the 'go' cue because of competition with the saccade target in the opposite hemifield, we added a control condition in which both the saccade target and the 'go' cue were in the neuron's response field. The pattern of neural activity in this condition (**Fig. 5c**, right) was virtually indistinguishable from the activity when the saccade target was presented in the RF and the 'go' cue outside the response field (green in **Fig. 5c**, left). Hence the location of the 'go' cue did not seem to influence the pattern of anticipation responses in LIP.

Based on these control experiments, we conclude that anticipatory modulation was strongest in LIP neurons that represent the locus of the intended eye movement.

DISCUSSION

We trained rhesus monkeys to anticipate the timing of a 'go' signal in a delayed saccade task. Unlike in previous studies[29], the monkeys had to learn two probabilistic time schedules that were used in alternating blocks of trials. To maximize the chances that the animals would learn both schedules, we used a bimodal and unimodal distribution of 'go' times with minimal overlap. Examination of the monkeys' reaction times demonstrated that they had learned features of these probabilistic schedules in order to anticipate the time of the 'go' instruction.

We also found that single neurons in area LIP modulated their firing rate as a function of time in a way that reflected the monkeys' state of anticipation. The spike rate was strongly influenced by the probability that the 'go' instruction would occur in the next moment, based on the monkey's experience with the two schedules. The spike rate modulation in LIP is thus related to the hazard rates associated with the unimodal and bimodal probabilistic schedules of 'go' times (**Figs 3** and **5**). The pattern of modulation also reflected the well-known fact that the experience of elapsed time carries with it a degree of uncertainty that is proportional to the true duration (Weber's law)[3,5,30]. This uncertainty implies that the distribution of 'go' times that the monkey experienced during training is a distorted version of the probability distributions that we programmed into the computer, giving rise to the subjective hazard rates reflected in LIP.

Notably, the temporal pattern of the LIP spike rate often changes substantially within a single experimental session upon a change in the probabilistic schedule. It is important to bear in mind that markedly different patterns of response (in **Fig. 3**, for example) were observed from the same neuron while the monkey viewed the identical display and awaited the 'go' instruction. Evidently, the brain can detect the change of schedule after a few samples of 'go' times (<30 trials) and adjusts its circuitry to achieve the appropriate pattern of anticipation in LIP. Further studies are needed to clarify the mechanism of this flexibility.

In the control experiment used to dissociate an intention to move the eyes from the spatial attention allocated to the detection of the 'go' instruction (**Fig. 5**), we found that the representation of the hazard rate was markedly diminished when the 'go' cue was in the response field and the saccade target was not. At first glance, this seems to contradict a recent study that demonstrated hazard-like modulation of attention-related signals in area V4 of the monkey[29]. However, a small amount of modulation was present when spatial attention was directed to the LIP response field (~5 spikes s^{-1} per unit of anticipation). It is possible that this is sufficient to explain the modest degree of modulation seen in the V4 study of attention. Alternatively, the allocation of spatial attention may be difficult to dissociate from an intention to make an eye movement[31]. Indeed, the neural basis of attention-related modulation in area V4 may be mediated through high-level oculomotor structures[32]. It is therefore plausible that the intention-related signals seen in our experiments could underlie a shift in spatial attention that is not in competition with an eye movement plan[33].

The present study cannot determine whether the timing-related anticipatory activity arises in area LIP or is simply passed to LIP from other structures that have been implicated in interval timing, such as the prefrontal cortex[18,20], the basal ganglia[34] or the cerebellum[35]. However, two observations lead us to suspect that the anticipation signals measured in LIP may have more than a coincidental role in shaping the monkey's behavior. First, the anticipation functions are reflected by the neurons and by the reaction time at the same latency with respect to the 'go' instruction. The anticipation of the 'go' instruction best matches the neural responses with a latency of 55 ms and is maximally (inversely) correlated with the monkey's reaction time 56 ms before the 'go' signal (**Fig. 2**).

Second, we observed a weak correlation between the variable responses on single trials and the monkey's reaction time (**Fig. 4**). The weakness of the reaction time–spike rate correlation distinguishes LIP from motor structures, such as the frontal eye field and the superior colliculus, with which it is interconnected[36,37]. Indeed, much larger negative correlations between spike rate and reaction time have been reported in these areas[38,39]. The weak correlation between the variable spike rate from LIP neurons on single trials and the monkey's subsequent reaction time on that trial suggests that either LIP neurons directly influence reaction time, or they mirror with great fidelity the structures that lie along the causal chain. This implies that the marked anticipation-related modulation represented in LIP is likely to explain the behavioral manifestation of anticipation: reduced saccadic latency.

Our findings extend a previous study that has demonstrated a possible role for area LIP in interval timing[5]. As in the present study, LIP neurons were found to encode the salience of potential eye movement targets in a dynamic fashion. In that study, the monkey's perception of the duration of a test light was explained by comparing the activity of LIP neurons whose activity increased or decreased as a function of time. In light of the present findings, we suspect that the modulation of activity is governed by the anticipation of the termination of the test light, whose random durations resemble the unimodal schedule of 'go' times used in the present study. By adding and subtracting the subjective hazard rate to or from low and high background firing rates, respectively, LIP could produce a pair of crisscrossing functions (as in ref. 5) to represent elapsed time with respect to a memorized standard duration.

Together, these studies suggest that LIP encodes elapsed time insofar as it affects the meaningfulness of visual objects that are potential gaze targets. Indeed, the observation that some LIP neurons track the motion of occluded objects[40] might be explained by the prediction of a salient object emerging from behind an occluder in time. In addition to elapsed time, it has been shown that persistent neural activity in area LIP can

be influenced by a variety of factors associated with reward expectation[12], response bias[41] and decision formation[42]. All of these functions require the neurons to operate on a time scale governed neither by immediate changes in the sensory environment nor by real-time constraints of moving body parts. Hence, the brain must keep an internal representation of time to determine by what time an action must occur or when information becomes relevant. Throughout the association cortex[4,20,43,44], neurons with persistent activity may therefore represent elapsed time to infer the temporal structure of the environment.

METHODS

Task. Two rhesus monkeys were trained on the delayed eye movement task[45]. The monkeys maintained their gaze within 1° of a fixation spot in the center of the display. After 400 ms of stable fixation, a red target was presented at a position between 3° and 15° eccentricity. After a variable delay, the fixation point dimmed by 30% of its luminance. This dimming served as the 'go' signal to make an eye movement to the target. A liquid reward was given for accurate saccades (within 4° of the target) initiated 150–500 ms after the 'go' signal. To encourage fast responses, reward size was governed by an exponential function of reaction time (minus 150 ms). The time between target onset and the 'go' signal was a random variable drawn from either a bimodal or a unimodal distribution (**Fig. 1b**, upper row). The bimodal distribution, $B(t)$, was the sum of two non-overlapping Rayleigh distributions, delayed by d_1 and d_2:

$$B(t) = \frac{1}{2}(R_1 + R_2)$$

where

$$R_i = \begin{cases} 2\alpha_i(t-d_i)e^{-\alpha_i(t-d_i)^2} & \text{for } t > d_i \\ 0 & \text{otherwise} \end{cases} \quad (1)$$

($\alpha_1 = 18$, $d_1 = 0.1$, $\alpha_2 = 15$, $d_2 = 1.75$). The 'go' time was drawn with equal probability from R_1 or R_2. The unimodal distribution of 'go' times was a single Weibull function delayed by 0.5 s:

$$U(t) = \begin{cases} 3\alpha(t-\frac{1}{2})^2 e^{-\alpha(t-\frac{1}{2})^3} & \text{for } t > \frac{1}{2} \\ 0 & \text{otherwise} \end{cases} \quad (2)$$

The probability distribution of the 'go' times was fixed throughout a block of trials. After 200–300 trials, the time schedule was changed without notification. Ideally, anticipation should be governed by the conditional probability that an event will occur given that it has not yet occurred, termed the hazard rate (**Fig. 1b**, middle row). This is the probability that the 'go' signal will occur at time t divided by the probability that it has not yet occurred:

$$h(t) = \frac{f(t)}{1 - F(t)} \quad (3)$$

where $f(t)$ is either $U(t)$ or $B(t)$, and $F(t)$ is the cumulative distribution, $\int_0^t f(s)ds$.

To obtain our predicted anticipation functions, we calculated 'subjective' hazard rates based on the assumption that elapsed time is known with uncertainty that scales with time. The probability density function $f(t) = U(t)$ or $B(t)$ was first blurred by a normal distribution whose standard deviation is proportional to elapsed time.

$$\tilde{f}(t) = \frac{1}{\phi t\sqrt{2\pi}} \int_{-\infty}^{\infty} f(t)e^{-(\tau-t)^2/(2\phi^2 t^2)}d\tau \quad (4)$$

The coefficient of variation, ϕ, is a Weber fraction for time estimation (for most analyses, $\phi = 0.26$). Equation (4) implements the idea that the monkey's estimate of elapsed time carries uncertainty. Thus, an event at objective time t_0 is sensed as if it occurred at $t_0 \pm \sigma$. The subjective hazard rate is then obtained by substituting $\tilde{f}(t)$ and its definite integral, $\tilde{F}(t)$ into equation (3). We refer to these subjective hazard rates as anticipation functions, $A_u(t)$ and $A_b(t)$, below. For ease of interpretation, they are scaled in all graphs and fits by a common factor (2.03, for $\phi = 0.26$) so that the functions range from 0 to 1 (**Fig. 1b**, bottom row).

In the cue experiment, a blue and a green stimulus were presented on opposite sides of the fixation point. The monkeys' task was to make a saccade to the green stimulus (the target) as soon as the blue stimulus (the cue) dimmed. We compared the activity during trials in which the 'go' cue was in the neuron's response field and the target was outside the response field, to trials in which the opposite configuration was present. To determine any potential color selectivity[46] we also recorded trials in which the monkey made saccades to either a green or a blue target in interleaved blocks of trials.

Recording procedure. Action potentials from single neurons were recorded extracellularly using standard procedures[10] and stored with 1 ms precision. Eye position was monitored using a scleral search coil (sampled at 1 kHz). We screened neurons using a memory-guided saccade task[45]. Only neurons with high spatially selective delay period activity were studied: the average delay activity (computed 320–720 ms after target onset) was at least 60% of the visual response (80–320 ms after target onset). Most of these neurons also showed strong presaccadic activity (88% had larger responses in a 100 ms epoch ending at saccade initiation than in the 300 ms epoch preceding this; $P < 0.05$, t-test). This property is typical of LIP neurons in other studies[10,24,37,47]. All training, surgical and recording procedures complied with the guidelines of the National Institutes of Health and the research protocols approved by the University of Washington.

Data analysis. For each trial, the spike rates were truncated at 50 ms after the dimming of the fixation point. The first 50 trials after the change in the time schedule were excluded from the analysis. We fitted the mean spike rates (80-ms bins) after the initial visual response (starting at 160 ms after target onset) using a weighted sum of subjective hazard rates:

$$r(t) = w_e + w_u A_u(t-\tau) + w_b A_b(t-\tau) + \varepsilon \quad (5)$$

where r is the neuronal response, w_e is a constant term, and w_u and w_b are the weights for the unimodal (A_u) and bimodal (A_b) anticipation functions, respectively, delayed by time shift τ. ε represents noise, which is assumed to be Gaussian with uncertainty derived from the sample means. Equation (5) was also used to fit the reaction times on each trial with a weighted sum of subjective hazard rates. Because the functions range from 0 to 1, the weights can be interpreted as the magnitude of the spike rate modulation attributed to these theoretical waveforms (an approximation to a basis set) in units of spikes per second per unit anticipation (for the fits to the reaction times, the units are milliseconds per unit anticipation).

We used a maximum-likelihood fitting procedure to obtain the fits, parameter estimates and their standard errors. Standard errors of parameters were estimated from the Hessian matrix of second partial derivatives of the log likelihood[48] and were used to generate t-statistics cited throughout the paper. We fit the data from each neuron and each schedule independently to obtain the weights shown in the scatter plots (**Fig. 3c**). The Weber fraction was fixed (equation (4), $\phi = 0.26$). We tried to estimate ϕ using the fits, but found that only strongly modulated neurons gave reliable estimates (mean ϕ from 48 reliable cases was 0.33 ± 0.03). A similar strategy was used to fit the population response data (**Fig. 3b**) except that fits to the two response averages were constrained to use a common time delay, τ, and the Weber fraction was free. The large Weber fraction obtained from these fits (0.41 and 0.5 for monkeys J and H, respectively) was probably induced by smearing of the response functions because of averaging. For the all other analyses, we assumed $\phi = 0.26$, consistent with previous human and animal studies[30,49] and with behavioral measurements in monkeys in our laboratory[5].

The partial correlation coefficients between the theoretical anticipation function and the reaction times (RT) observed under either the unimodal or bimodal schedule were calculated by partitioning the 3×3 covariance matrix based on the ordered triplets $[RT(t), A_u(t-\tau), A_b(t-\tau)]$, where t is the 'go' time and $\tau = 56$ ms (from the fit shown in **Fig. 2**). The partitioning effectively factors out the contribution of the potentially confounding variable (for example, $A_u(t-\tau)$ for data obtained with the bimodal schedule) on the correlation between the other two variables[50].

For the spatial control experiment (**Fig. 5**), we also tested for color selectivity by interleaving blocks of trials in which the monkey made saccades to either a green or a blue target. Only 2 of 18 neurons responded significantly more to one color. The mean absolute response difference between the two colors was 3.6 spikes s^{-1} (s.d. = 4.0, which is >0.75 times the mean, consistent with the expected distribution of absolute values under hypothesis H_0: no difference).

ACKNOWLEDGMENTS

We thank M. Mihali and L. Jasinski for technical assistance, and T. Yang, T. Hanks, M. Leon and J. Palmer for helpful comments on the manuscript. Work was supported by Howard Hughes Medical Institute, the International Human Frontiers Science Program Organization, the Fonds voor Wetenschappelijk Onderzoek Vlaanderen, the National Center for Research Resources (RR00166) and the National Eye Institute (EY11378).

COMPETING INTERESTS STATEMENT

The authors declare that they have no competing financial interests.

Received 17 September; accepted 20 December 2004
Published online at http://www.nature.com/natureneuroscience/

1. Gallistel, C.R. & Gibbon, J. Time, rate and conditioning. *Psychol. Rev.* **107**, 289–344 (2000).
2. Mauk, M.D. & Buonomano, D.V. The neural basis of temporal processing. *Annu. Rev. Neurosci.* **27**, 307–340 (2004).
3. Meck, W.H. Internal clock and reward pathways share physiologically similar information-processing pathways. in *Quantitative Analyses of Behavior: Biological Determinants of Reinforcement* vol. 7 (eds. Commons, M.L., Church, R.M., Stellar, J.R. & Wagner, A.R.) 121–138 (Erlbaum, Hillsdale, New Jersey, USA, 1988).
4. Coull, J.T. & Nobre, A.C. Where and when to pay attention: the neural systems for directing attention to spatial locations and to time intervals as revealed by both PET and fMRI. *J. Neurosci.* **18**, 7426–7435 (1998).
5. Leon, M.I. & Shadlen, M.N. Representation of time by neurons in the posterior parietal cortex of the macaque. *Neuron* **38**, 317–327 (2003).
6. Onoe, H. *et al.* Cortical networks recruited for time perception: a monkey positron emission tomography (PET) study. *Neuroimage* **13**, 37–45 (2001).
7. Funahashi, S., Chafee, M.V. & Goldman-Rakic, P.S. Prefrontal neuronal activity in rhesus monkeys performing a delayed anti-saccade task. *Nature* **365**, 753–756 (1993).
8. Tanji, J. & Hoshi, E. Behavioral planning in the prefrontal cortex. *Curr. Opin. Neurobiol.* **11**, 164–170 (2001).
9. Andersen, R.A. & Buneo, C.A. Intentional maps in posterior parietal cortex. *Annu. Rev. Neurosci.* **25**, 189–220 (2002).
10. Shadlen, M.N. & Newsome, W.T. Neural basis of a perceptual decision in the parietal cortex (area LIP) of the rhesus monkey. *J. Neurophysiol.* **86**, 1916–1936 (2001).
11. Schall, J.D. Neural correlates of decision processes: neural and mental chronometry. *Curr. Opin. Neurobiol.* **13**, 182–186 (2003).
12. Platt, M.L. & Glimcher, P.W. Neural correlates of decision variables in parietal cortex. *Nature* **400**, 233–238 (1999).
13. Karlin, L. Development of readiness to respond during short foreperiods. *J. Exp. Psychol.* **72**, 505–509 (1966).
14. Luce, R.D. *Response Times: Their Role in Inferring Elementary Mental Organization* (Oxford Univ. Press, New York, 1986).
15. Schall, J.S. & Hanes, D.P. Saccade latency in context: regulation of gaze behavior by supplementary eye field. *Behav. Brain Sci.* **16**, 588–589 (1993).
16. Basso, M.E. & Wurtz, R.H. Modulation of neuronal activity by target uncertainty. *Nature* **389**, 66–69 (1997).
17. Dorris, M.C. & Munoz, D.P. Saccadic probability influences motor preparation signals and time to saccadic initiation. *J. Neurosci.* **18**, 7015–7026 (1998).
18. Niki, H. & Watanabe, M. Prefrontal and cingulate unit activity during timing behavior in the monkey. *Brain Res.* **171**, 213–224 (1979).
19. Chafee, M.V. & Goldman-Rakic, P.S. Matching patterns of activity in primate prefrontal area 8a and parietal area 7ip neurons during a spatial working memory task. *J. Neurophysiol.* **79**, 2919–2940 (1998).
20. Brody, C.D., Hernandez, A., Zainos, A. & Romo, R. Timing and neural encoding of somatosensory parametric working memory in macaque prefrontal cortex. *Cereb. Cortex* **13**, 1196–1207 (2003).
21. Reutimann, J., Yakovlev, V., Fusi, S. & Senn, W. Climbing neuronal activity as an event-based cortical representation of time. *J. Neurosci.* **24**, 3295–3303 (2004).
22. Durstewitz, D. Neural representation of interval time. *Neuroreport* **15**, 745–747 (2004).
23. Loveless, N.E. & Sanford, A.J. Slow potential correlates of preparatory set. *Biol. Psychol.* **1**, 303–314 (1974).
24. Bracewell, R.M., Mazzoni, P., Barash, S. & Andersen, R.A. Motor intention activity in the macaque's lateral intraparietal area. II. Changes of motor plan. *J. Neurophysiol.* **76**, 1457–1464 (1996).
25. Gnadt, J.W. & Andersen, R.A. Memory related motor planning activity in posterior parietal cortex of macaque. *Exp. Brain Res.* **70**, 216–220 (1988).
26. Colby, C.L. & Goldberg, M.E. Space and attention in parietal cortex. *Annu. Rev. Neurosci.* **22**, 319–349 (1999).
27. Lewis, J.W. & Van Essen, D.C. Mapping of architectonic subdivisions in the macaque monkey, with emphasis on parieto-occipital cortex. *J. Comp. Neurol.* **428**, 79–111 (2000).
28. Bisley, J.W. & Goldberg, M.E. Neuronal activity in the lateral parietal area and spatial attention. *Science* **299**, 81–86 (2003).
29. Ghose, G.M. & Maunsell, J.H.R. Attentional modulation in visual cortex depends on task timing. *Nature* **419**, 616–620 (2002).
30. Gibbon, J., Malapani, C., Dale, C.L. & Gallistel, C.R. Toward a neurobiology of temporal cognition: advances and challenges. *Curr. Opin. Neurobiol.* **7**, 170–184 (1997).
31. Rizzolatti, G., Riggio, L., Dascola, I. & Umilta, C. Reorienting attention across the horizontal and vertical meridians: evidence in favor of a premotor theory of attention. *Neuropsychologia* **25**, 31–40 (1987).
32. Moore, T. & Armstrong, K.M. Selective gating of visual signals by microstimulation of frontal cortex. *Nature* **421**, 370–373 (2003).
33. Kowler, E., Anderson, E., Dosher, B. & Blaser, E. The role of attention in the programming of saccades. *Vision Res.* **35**, 1897–1916 (1995).
34. Rao, S.M., Mayer, A.R. & Harrington, D.L. The evolution of brain activation during temporal processing. *Nat. Neurosci.* **4**, 317–323 (2001).
35. Ivry, R.B. & Spencer, R.M.C. The neural representation of time. *Curr. Opin. Neurobiol.* **14**, 225–232 (2004).
36. Ferraina, S., Pare, M. & Wurtz, R. Comparison of cortico-cortical and cortico-collicular signals for the generation of saccadic eye movements. *J. Neurophysiol.* **87**, 845–858 (2002).
37. Pare, M. & Wurtz, R.H. Monkey posterior parietal cortex neurons antidromically activated from superior colliculus. *J. Neurophysiol.* **78**, 3493–3497 (1997).
38. Dorris, M.C., Pare, M. & Munoz, D.P. Neuronal activity in monkey superior colliculus related to the initiation of saccadic eye movements. *J. Neurosci.* **17**, 8566–8579 (1997).
39. Everling, S. & Munoz, D.P. Neuronal correlates for preparatory set associated with pro-saccades and anti-saccades in the primate frontal eye field. *J. Neurosci.* **20**, 387–400 (2000).
40. Eskandar, E.N. & Assad, J.A. Dissociation of visual, motor and predictive signals in parietal cortex during visual guidance. *Nat. Neurosci.* **2**, 88–93 (1999).
41. Coe, B., Tomihara, K., Matzuzawa, M. & Hikosaka, O. Visual and anticipatory bias in three cortical eye fields of the monkey during an adaptive decision-making task. *J. Neurosci.* **22**, 5081–5090 (2002).
42. Shadlen, M.N. & Newsome, W.T. Motion perception: seeing and deciding. *Proc. Natl. Acad. Sci. USA* **93**, 628–633 (1996).
43. Roux, S., Coulmance, M. & Riehle, A. Context-related representation of timing processes in monkey motor cortex. *Eur. J. Neurosci.* **18**, 1011–1016 (2003).
44. Coull, J.T., Vidal, F., Nazarian, B. & Macar, F. Functional anatomy of the attentional modulation of time estimation. *Science* **303**, 1506–1508 (2004).
45. Hikosaka, O. & Wurtz, R. Visual and oculomotor functions of monkey substantia nigra pars reticulata. III. Memory-contingent visual and saccade responses. *J. Neurophysiol.* **49**, 1268–1284 (1983).
46. Toth, L.J. & Assad, J.A. Dynamic coding of behaviourally relevant stimuli in parietal cortex. *Nature* **415**, 165–168 (2002).
47. Colby, C. L., Duhamel, J.-R., & Goldberg, M. E. Visual, presaccadic, and cognitive activation of single neurons in monkey lateral intraparietal area. *J. Neurophysiol.* **76**, 2841–2852 (1996).
48. Meeker, W.Q. & Escobar, L.A. *Statistical Methods for Reliability Data* (Wiley, New York, 1998).
49. Rakitin, B.C. *et al.* Scalar expectancy theory and peak-interval timing in humans. *J. Exp. Psychol. Anim. Behav. Process.* **24**, 15–33 (1998).
50. Anderson, T.W. An Introduction to Multivariate Statistical Analysis edn. 2 (Wiley, New York, 1984).